An Organic Bifunctional Redox Active Material for Symmetric Aqueous Redox Flow Battery

Gabriel Sikukuu Nambafu [a], Kumar Siddharth [a], Cheng Zhang [b,c], Tianshou Zhao [b,c], Qing Chen [b,c], Khalil Amine [d,e,f,*], Minhua Shao [a,c,*]

[a] Department of Chemical and Biological Engineering, The Hong Kong University of Science and Technology, Clear Water Bay, Kowloon, Hong Kong

[b] Department of Mechanical and Aerospace Engineering, The Hong Kong University of Science and Technology, Clear Water Bay, Kowloon, Hong Kong

[c] Energy Institute, The Hong Kong University of Science and Technology, Clear Water Bay, Kowloon, Hong Kong

[d] Chemical Sciences and Engineering Division, Argonne National Laboratory, 9700 South Cass Avenue, Lemont, II, 60439, United States

e Materials Science and Engineering, Stanford University, Stanford, California 94305, United States

f Institute for Research and Medical Consultations (IRMC), Imam Abdulrahman Bin Faisal University (IAU), Dammam 34221, Saudi Arabia

[*]Corresponding authors: amine@anl.gov; kemshao@ust.hk

Abstract

Symmetric redox flow batteries utilizing a single redox active material as catholyte and anolyte, offer a plausible and unique strategy to alleviate cross-contamination issues during cycling, making them an ideal energy storage device for large scale applications. In this work, a low-cost riboflavin organic molecule is coupled with a 2,2,6,6-Tetramethylpiperidinyl-N-oxyl (TEMPO) radical molecule to form a single Riboflavin-TEMPO (RIBOTEMPO) bifunctional redox active material, which is used in both aqueous anolyte and catholyte. Cyclic voltammetry analysis of the combined molecule displays electrochemically reversible reactions for the redox couples at -0.72 V and 0.51 V versus Hg/Hg_2SO_4, leading to a theoretical cell voltage of 1.23 V. A symmetric cell testing demonstrated over 100 consecutive charge/discharge cycles with nearly 80% coulombic efficiency and capacity retention of 44.7% at a current density of 2.5 mA cm^{-2}. By utilizing a pH neutral supporting electrolyte, a low-cost, safe, and environmental-friendly redox flow battery is achieved. This work provides a pathway for the design and development of bifunctional redox active molecules for symmetric battery applications.

Keywords: Energy storage; symmetric aqueous redox flow battery; redox active materials; bipolar organic molecules

1. Introduction

Renewable energy technologies are expected to provide an alternative clean energy to replace fossil fuels. This trend is initiated by environmental concerns associated with energy sources emitting harmful and greenhouse gases and energy security issues triggered by the ever-increasing energy demand [1]. Moreover, most renewable energy systems are intermittent and have a fluctuating nature that causes discrepancies between power supply and demand, hindering their reliability [2]. In this regard, the development of large-scale energy storage technologies is essential to widely support the renewable energy sources. Owing to their unique feature of scalable and decoupled power and energy densities, redox flow batteries (RFBs) have shown great potential for large scale energy storage applications [3,4,5].

Over the past ten years, the urge to develop a high-performance RFB has prompted a massive investigation on inorganic, organic and organometallic materials, racing towards identifying a suitable redox active material [6,7,8]. Commercialization and further development of traditional RFBs based on metal electrolytes have been confronted by many challenges such as use of toxic/non-eco-friendly electrolyte, slow reaction kinetics of the redox couples, high cost, along with low energy and power densities compared to conventional secondary batteries [9,10]. On the other hand, organic RFBs have shown potentials to overcome these challenges, owing to their unique characteristics such as low cost, high solubility, and environment friendliness. In addition, organic molecules exist in diverse molecular structures, that facilitates synthetic tunability to design suitable molecules with the desired physical and electrochemical properties [11].

Different types of organic electroactive materials have been demonstrated as anolyte and catholytes in asymmetric RFBs, which is the most common design [8,10,11]. Nonetheless, asymmetric RFBs design based on two different organic molecules as respective anolyte and catholyte still experience cross-contamination issues. This causes capacity loss during cycling, making them unviable [12]. Among the various inorganic and organic RFB technologies already investigated, all-vanadium RFB remains the most studied and developed chemistry. This is due to the fact that it employs all-vanadium redox species as anolyte and catholyte, mitigating cross-contamination issues during cycling. However, expensive vanadium metal, highly corrosive supporting electrolyte as well as low energy density resulting from low

solubility of vanadium species, have decelerated commercialization of this technology [10,13]. Henceforth, replacing vanadium electroactive species with tuneable organic redox active materials with bifunctional/bipolar properties will be a big step towards advancing the symmetric RFBs technologies.

Mimicking all-vanadium redox flow battery technology, researchers have been working on developing symmetric organic RFBs, utilizing either aqueous or non-aqueous supporting electrolyte. The already studied organic molecules for symmetric RFBs chemistry are, diaminoanthraquinone [14,15], verdazyl radical [16], porphyrins [17], nitronyl nitroxide radical [18], benzoyl pyridinium derivative [19] for non-aqueous systems and 2,2,6,6-Tetramethylpiperidinyl-N-oxyl (TEMPO)/Phenazine combi-molecule [20], 1-(4-(((1-oxyl-2.2.6.6-tetramethylpiperidin-4-yl)oxy)carbonyl)benzyl)-1'-methyl-[4,4'-bipyridine]-1,1'-diium-chloride (VIOTEMP) [21] for aqueous systems. Aqueous RFB systems are considered the most promising for a safe and low-cost large scale energy storage device. Nevertheless, most organic redox active materials either have low solubility or low stability in aqueous solution [22]. Therefore, there is a need to introduce new RFBs chemistry/electroactive molecules to provide a wide range of water-soluble redox active materials for application in symmetric aqueous RFBs [23].

In this work, we report a Riboflavin-TEMPO (RIBOTEMPO) combined molecule with bifunctional properties for application in symmetric flow batteries. Riboflavin and TEMPO are commercially available molecules and have been investigated previously as potential anolyte and catholyte respectively in asymmetric redox flow batteries by virtue of their fast, stable, and reversible redox reactions [24,25,26]. Herein, the two molecules were combined via a simple one pot synthesis method to form a single redox molecule that demonstrated improved electrochemical properties. The bifunctional redox active material was electrochemically characterized and its performance in a pumped RFB was investigated. It demonstrated a cell voltage of 1.23 V and a capacity retention of 44.7% after 100 charge/discharge cycles at a current density of 2.5 mA cm^{-2}. Furthermore, it should be noted that besides helping evade cross-contamination issues, combining molecules also provides an avenue for introducing different functional groups into an organic molecule i.e., functionalization of organic molecule, thus enhancing their electrochemical properties [23,27,28]. Therefore, this work provides an insight and pathway towards replacing the expensive metal based RFBs, through design and synthesis of bifunctional/bipolar water-soluble redox active material for application in aqueous symmetric batteries.

2. Experimental

2.1.Chemicals and Materials

Riboflavin sodium phosphate ($C_{17}H_{20}N_4NaO_9P$, 93%, Aladdin, China), 4-Amino-2,2,6,6-tetramethylpiperidine 1-Oxyl ($C_9H_{19}N_2O$, 97%, Aladdin, China), silicotungstic acid hydrate ($H_3PW_{12}O_{40} \geq 99.9\%$, Millipore Sigma), formaldehyde (HCHO, 37% in H_2O, Sigma Aldrich), hydrochloric acid (HCl, 37%, Sigma Aldrich), sodium chloride ($NaCl \geq 99.0\%$, Sigma Aldrich) were purchased and used as received without any purification. Nitrogen (N_2) and Argon (Ar) gases were used for protection of all oxygen sensitive reactions.

2.2. Organic synthesis

The RIBOTEMPO combined molecule was synthesized via the Mannich reaction by modifying procedures in previous reported literatures [29,30,31]. The synthesis route is also shown in Figure S1. Riboflavin sodium phosphate (3 mmol), 4-Amino TEMPO (3 mmol) and formaldehyde (3 mmol) were added in a flask containing silicotungstic acid hydrate (15 mg) as catalyst in water (50 ml) and vigorously stirred and refluxed at 80°C for 24 hrs. The resulting mixture was then cooled and diluted to 100 ml with distilled water and treated with 3 M HCl (20 ml) and set aside overnight. The precipitate was filtered off and the filtrate extracted with ethanol-ether and dried at 70 °C under vacuum to afford the product.

The product was determined through matrix-assisted laser desorption/ionization-time of flight (MALDI-TOF) mass spectra performed on a Water Q-TOF (LC-MS) mass spectrometer and H NMR. pH measurements were taken using an HINOTEK portable pH meter (PHBJ-260). Calibration of the pH meter was done at room temperature using Certipur® pH 4 (107200) & pH 7 (107205) reference buffer solutions.

2.3.Electrochemical characterizations

Cyclic voltammetry (CV) and linear sweep voltammetry (LSV) measurements in 3 mM RIBOTEMPO combined molecule + 0.1 M NaCl were performed using an electrochemical working station controlled by a potentiostat from CH instruments (CHI 760 or 627e). Both measurements were carried out in a three-electrode glass cell using glassy carbon electrode as the working electrode (5 mm diameter), Pt wire as the counter electrode and Hg/Hg_2SO_4

electrode as the reference electrode. The glassy carbon electrode was polished using Al_2O_3 paste, then suspended in deionised water, rinsed and dried before use. The measurements were carried out at room temperature with a continuous flow of argon gas into the cell to create an inert atmosphere. The CV Measurements were conducted at the scan rate of 50 mV s^{-1} between -1.0 V and 0.8 V. The scans were done 200 times continuously at 50 mV s^{-1} to evaluate the stability of the molecule during CV analysis. Different scan rates at 100, 200, 300, 400 and 500 mV s^{-1} were also recorded. The scanning experiments were repeated 6 times at each scan rate to ensure accuracy. The LSV measurements were done at a scan rate of 5 mV s^{-1} between -1.7 V and 1.0 V. The electrode was rotated using Pine research modulated speed rotator (AFMSRCE 2252) at a rate of 100 to 2000 rpm. The LSV data were analysed using Levich plots, thereafter the diffusion coefficient and rate constant of the RIBOTEMPO molecule were calculated.

2.4. Flow battery assembly

The battery was assembled using a redox flow cell stack hardware that was designed and constructed by Shanghai SHIMATOYO Electronics Co., Ltd (China). The cell stack had the serpentine flow field (SFF) design with a membrane and electrode active area of 4 cm^2. A fumasep® FAA-3-50 (Fuel Cell Store, USA) anion-exchange membrane was employed as the separator, and graphite felt (2×2×0.6 cm, GFA6, SGL Carbon SE, Germany) was used as the electrode. The membrane was cut into suitable size and pre-treated before use. Pre-treatment was done by soaking the membrane in 2 M NaCl solution for 24 hrs to convert it into Cl^- form from the original Br^- form. A solution of NaCl was prepared containing the redox active material (RIBOTEMPO molecule) and used as the electrolyte. 20 ml of the electrolyte was placed in two bottles, then purged with nitrogen gas for 1 hr and employed as posolyte and negolyte during battery cycling. The electrolytes were pumped from the storage tank to the electrochemical cell stack at a rate of 60 rpm controlled by a peristaltic pump (Longer Pump WT600-2J). During battery testing, the charging and discharging process was carried at a constant current and specific charge and discharge cut-off voltages using a Neware battery testing system. To study the impact of cut-off voltage in the battery performance, different cut-off voltage ranges were used. The measurements were carried at room temperature (25 °C).

3. Results and Discussion

3.1.CV and LSV Analysis

The potentiality of the RIBOTEMPO combined molecule to be used as bipolar redox active molecule in a symmetric battery depends on the electrochemical availability and reversibility of different redox couples existing in different oxidation states. Therefore, the electrochemical properties of RIBOTEMPO combined molecule in 0.1 M NaCl was evaluated using CV and LSV first. To begin with, the CV analysis of individual molecules in comparison with the combined molecule was carried out as shown in Fig. 1a. The CV analysis of individual/separate TEMPO molecule displays the expected redox peaks with half redox potential at 0.52 V as well as an additional small anodic peak at 0.331 V vs. Hg/Hg_2SO_4. The small peak was attributed to oxidation of hydroxylamine form of TEMPO to TEMPO radical [32]. This oxidation mechanism proceeds as shown by the insertion in Fig.1a. Furthermore, CV of riboflavin exhibits anodic and cathodic peaks at -0.52 V and -0.75 V respectively generating the half potential at -0.64 V. Accordingly, CV analysis of RIBOTEMPO displayed two expected well defined redox couples, one at a lower potential zone and another at a higher potential zone. The potential interval between the two redox couples leads to a theoretical cell voltage of 1.23 V. Moreover, the combined molecule voltammogram shown in Fig. 1a, not only displays increase in the cathodic peak current of both redox couples, but also shows a negative shift by 132 mV for the anodic peak potential of the lower potential zone redox couple. This results in a smaller peak potential separation of 134 mV for combined molecule in comparison to 236 mV for individual/ separate riboflavin molecule, thus demonstrating improved reversibility. Therewithal, the reduction and oxidation mechanism of the redox couples is shown in Fig. 1b. The lower potential zone redox couple was associated with the riboflavin part of the combined molecule; it represents the oxidation/reduction via lose/gain of an electron and a proton by the nitrogen atoms situated in the alloxazine ring of the molecule [33]. This redox couple exhibited a half wave potential of -0.72 V versus Hg/Hg_2SO_4. The peak potential separation between the anodic peak potential (-0.653 V) and cathodic peak potential (-0.787 V) was 134 mV. On the other hand, the higher potential zone redox couple was associated with the TEMPO part of the combined molecule, representing the oxidation/reduction of nitroxide radical (TEMPO radical) to oxoammonium cation (TEMPO+) and vice-versa. The TEMPO/TEMPO+ redox couple showed a half wave potential of 0.51 V versus Hg/Hg_2SO_4. The additional anodic peak present in CV of individual TEMPO molecules dissipates in CV of the combined molecule, as the proton-dependent redox reaction of the riboflavin part favors direct oxidation of hydroxylamine species to oxoammonium cation [32]. Besides, the peak potential separation of the TEMPO/TEMPO+ redox couple between the anodic peak potential (0.554 V) and cathodic peak potential (0.468 V) was 86 mV. The peak-to-peak separation of both redox couples

indicates good kinetic reversibility. This is because both peak-to-peak separation values can be related to expected peak potential separation value for a reversible electron transfer system [34].

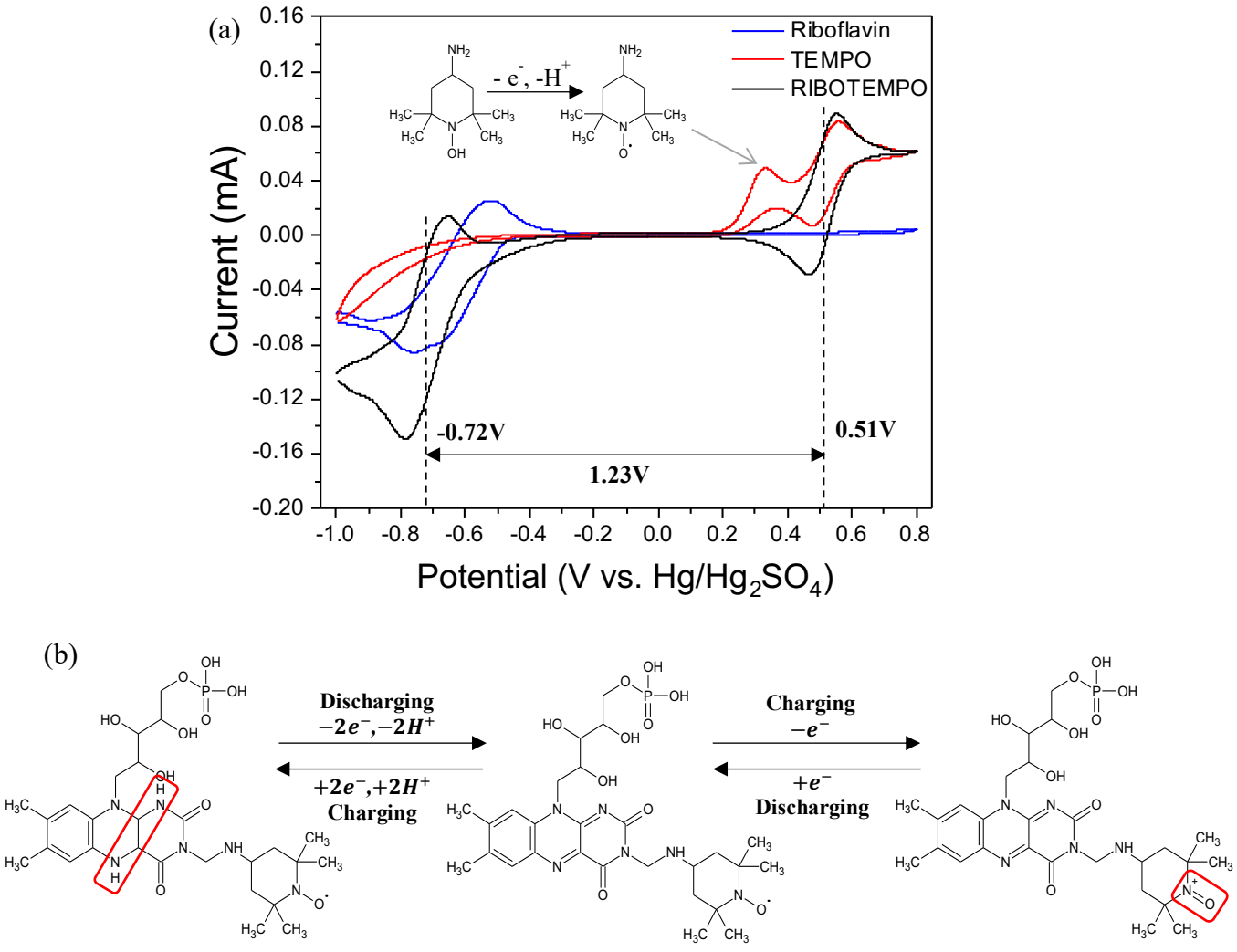

Fig. 1. Cyclic voltammetry of various organic molecules in 0.1 M NaCl at scan rate of 50 mV s^{-1} (a) riboflavin, TEMPO and RIBOTEMPO (b) redox mechanism of RIBOTEMPO molecule.

Fig. 2a shows the CV curves for the 1st - 200th cycles overlapping with each other, confirming electrochemical stability and reproducibility for both redox couples during CV scans. Scan rate dependence CV studies shows increase in peak currents with increase in scan rate, while the peaks potential displays negligible variation as shown in Fig. 2b. Randles-Sevcik's plot reveals a linear relationship between the current peaks and the square root of the scan rate as shown in Fig. 2c and Fig. 2d. This suggests that the redox process of both redox couples is diffusion controlled.

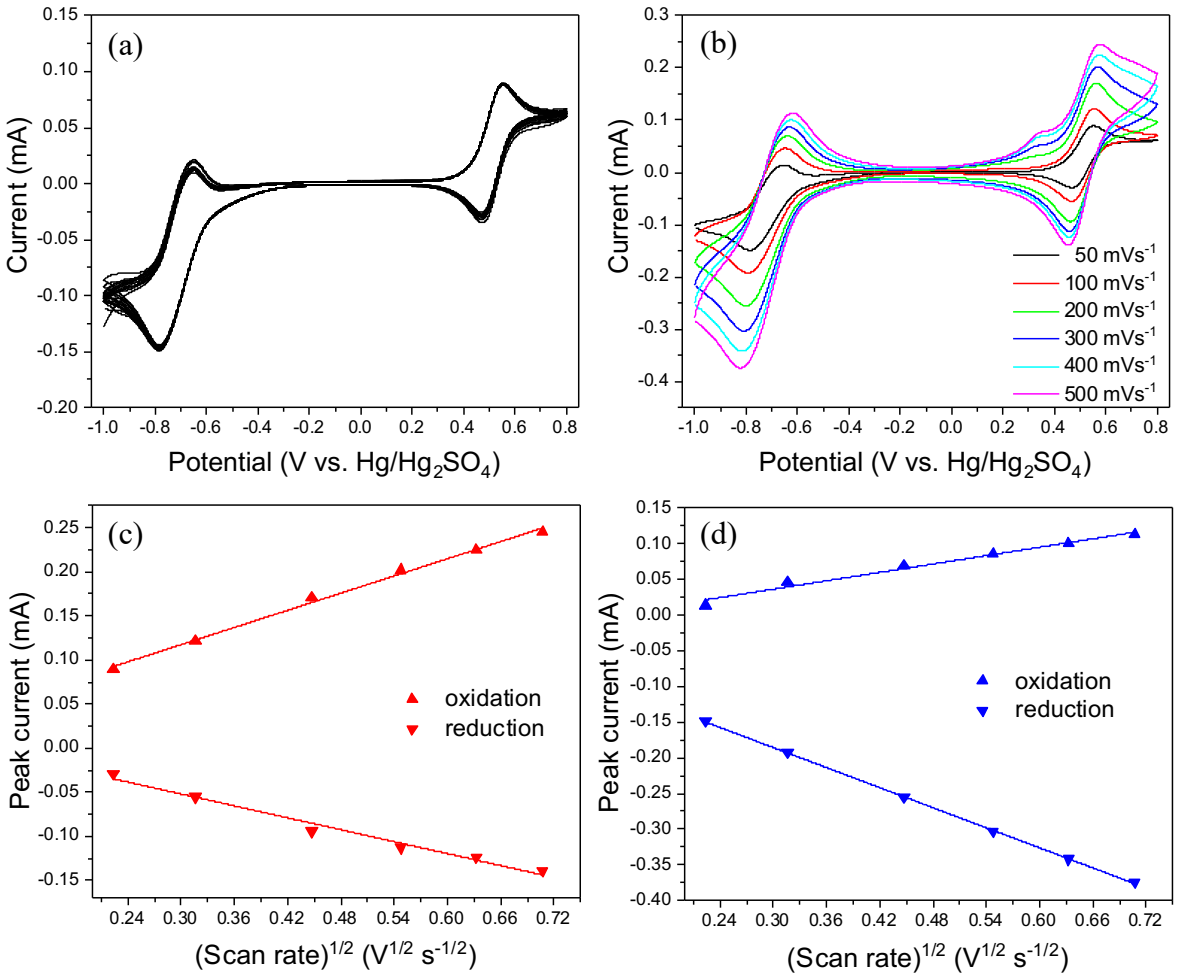

Fig. 2. Electrochemical characterization of RIBOTEMPO: (a) cyclic voltammetry for 200 cycles (b) cyclic voltammetry at varying scan rates, and plots of the oxidation and reduction current peaks the square root of the scan rate (c) lower potential redox couple (d) higher potential redox couple. (Condition: 3mM RIBOTEMPO in 0.1 M NaCl, scan rate 50 mV s^{-1}).

LSV measurements demonstrated well defined plateaus for both redox couples (Figure S2a and S2b). The limiting current at -1. 3 V (riboflavin part) and 0.7 V (TEMPO part) versus the square root of the rotation rates were plotted as shown in Figure S2c and straight Levich plots obtained with the slope defined by the Levich equation as follows [35]:

$$slope\ of\ the\ levich\ plot = 0.620\ nFAC_0\ D^{\frac{2}{3}}\upsilon^{-\frac{1}{6}},$$

with n = number of electrons transferred, Faraday's constant F = 96,485 C mol^{-1}, A = electrode surface of 0.196 cm^2, kinematic viscosity of the 0.1 M NaCl solutions ν = 1.0×10^{-2} cm^2 s^{-1} at 298.3 K and the C_0 = concentration of the redox-active material (3 mM). Using this equation, the calculated diffusion coefficients were 7.92×10^{-6} and 5.39 ×10^{-6} cm^2 s^{-1} for the riboflavin and TEMPO part of the molecule respectively. In comparison, the diffusion coefficients of individual riboflavin and TEMPO molecules were 3.85×10^{-6} and 6.52×10^{-6} cm^2 s^{-1} respectively (Figure S3) [36,37]. A plot of log i_k versus the overpotential as shown in Figure S2d was obtained using the LSV data collected at 1200 rpm for both parts of the RIBOTEMPO molecule. Thereafter, linear fitting produced Tafel plots representing each part (Riboflavin and TEMPO part). The x-intercept gave the logarithm of the exchange currents (i_k): 4.36×10^{-4} and 2.75×10^{-4} A for the riboflavin and TEMPO parts, respectively. Finally, the rate constant k_0 was obtained according to equation $i_k = nFAk_oC$ which gives k_0 of 7.54×10^{-3} cm s^{-1} and 4.75×10^{-3} cm s^{-1} for riboflavin and TEMPO parts, respectively. The k_0 results obtained are comparable to those of already investigated organic molecules for RFBs applications [24]. It confirms feasibility for using this combined molecule as redox active material in the battery [38].

3.2.Flow Battery tests

To further investigate the energy storage capability of the RIBOTEMPO combined molecule, a redox flow battery was assembled employing the molecule as a bifunctional redox active material. The attained solubility of the combined molecule as shown in Figure S4a-c was 0.32 M in an aqueous solution resulting in an energy density of 7.03 Wh L^{-1}. The energy density of this battery is limited by the solubility of the RIBOTEMPO molecule in NaCl supporting electrolyte. Notwithstanding, the solubility was further improved by introducing nicotinamide in the supporting electrolyte. Nicotinamide is a hydrotropic agent which has been reported and employed to enhance the solubility of flavin based molecules [39,40,41,42]. The solubility was improved to 1.22 M leading to an energy density of 26.81 Wh L^{-1} (Figure S5). Noteworthily, addition of nicotinamide has no impact on redox processes of RIBOTEMPO as the peaks potential and current remain unchanged as shown in Figure S6 [24]. In this study, 20 ml of RIBOTEMPO molecule in NaCl was used as the electrolyte (both catholyte and anolyte) and circulated through the cell stack using the peristaltic pump. The battery testing was done at different current density and different charge and discharge cut-off voltages. The pH neutral

supporting electrolyte used was compatible with the low-cost anion exchange membrane, as it is non-toxic and non-corrosive. In addition, its electrochemical stability window is broad enough to avoid H_2 and O_2 evolution reactions [43]. The battery cycling process was easily monitored as both electrolytes display color change from the original yellow color during the charge/discharge process as shown in Figure S7. Negolyte displays a green color whereas the posolyte displays an orange color during cycling. Representative 5^{th} - 10^{th} cycles during battery testing between 0.6 and 1.65 V are shown in Figure S8a. The battery cycling performance in the same cut-off voltage window demonstrated over 100 consecutive charge/discharge cycles with a coulombic efficiency of around 80% as shown in Fig. 3b. Also, Fig. 3a shows the first charge and discharge plateau at around 1.2 V, which is similar to the theoretical voltage as evaluated by CV studies of RIBOTEMPO molecule. The first cycle reached a capacity of 1.562 mAh and decreased to 0.227 mAh at the 100^{th} cycle. The overall capacity retention after 100 cycles was 15 % in this potential window. It is worth noting that faster capacity fade was experienced within the first 14 cycles showing 50% capacity loss.

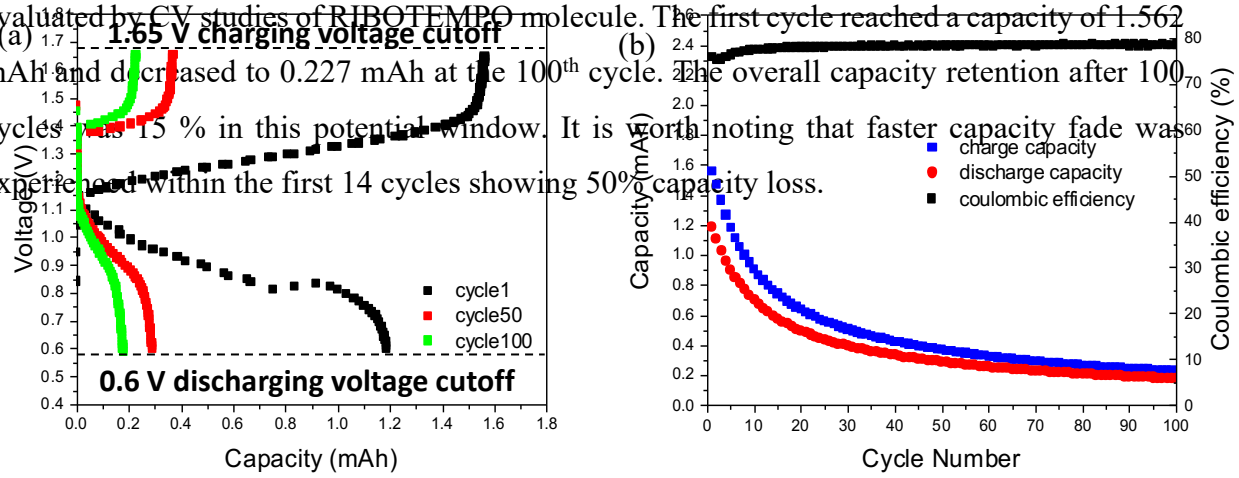

Fig. 3. Demonstration of full flow battery performance of 3 mM combined RIBOTEMPO molecule at current density of 2.5 mA cm^{-2}, charge cut-off voltage of 1.65 V and discharge cut-off voltage of 0.6 V (a) galvanostatic charge-discharge profiles during the 1^{st}, 50^{th}, and 100^{th} cycles, and (b) cycling performance and coulombic efficiencies.

To optimize the battery performance and investigate the impact of cut-off voltage on the flow battery performance, charge/discharge cycling was done at a narrower cut-off voltages range. Battery cycling at 1.0 -1.4 V demonstrated the best performance in terms of stability. An initial capacity of 1.709 mAh and first cycle's charge/discharge plateau around 1.2 V were exhibited as shown in Fig. 4a. Importantly, a much better capacity retention of 44.7% after 100 consecutive charge/discharge cycles was achieved with an average coulombic efficiency of

75% as shown in Fig. 4b. During this testing, voltage and energy efficiencies of 93% and 70% respectively were also achieved (Figure S8d). Supplementarily, battery cycling was explored at four different cut-off voltages with the intention of evaluating the effect of the cut-off voltage window on the stability of the RIBOTEMPO molecule. The battery testing revealed an initial capacity of 1655.4 mAh, coulombic efficiency of around 80% and capacity retention of 22% after 100 cycles for cut-off voltage range between 0.8 -1.4 V as shown in Fig. 4c & 4d. In addition, Fig. 4e & 4f displays an initial capacity of 1679.1 mAh, coulombic efficiency of 70% and capacity retention of 23% after 100 cycles at cut-off voltage range of 1.0 -1.6 V. Based on the various tests, decreasing the charge cut-off voltage, and increasing the discharge cut-off voltage, consequently narrowing the voltage window contributed to a better stability during cycling. Narrowing of the voltage window could have alleviated molecule degradation thus reducing capacity decay ascribable to active material decompositions [25].

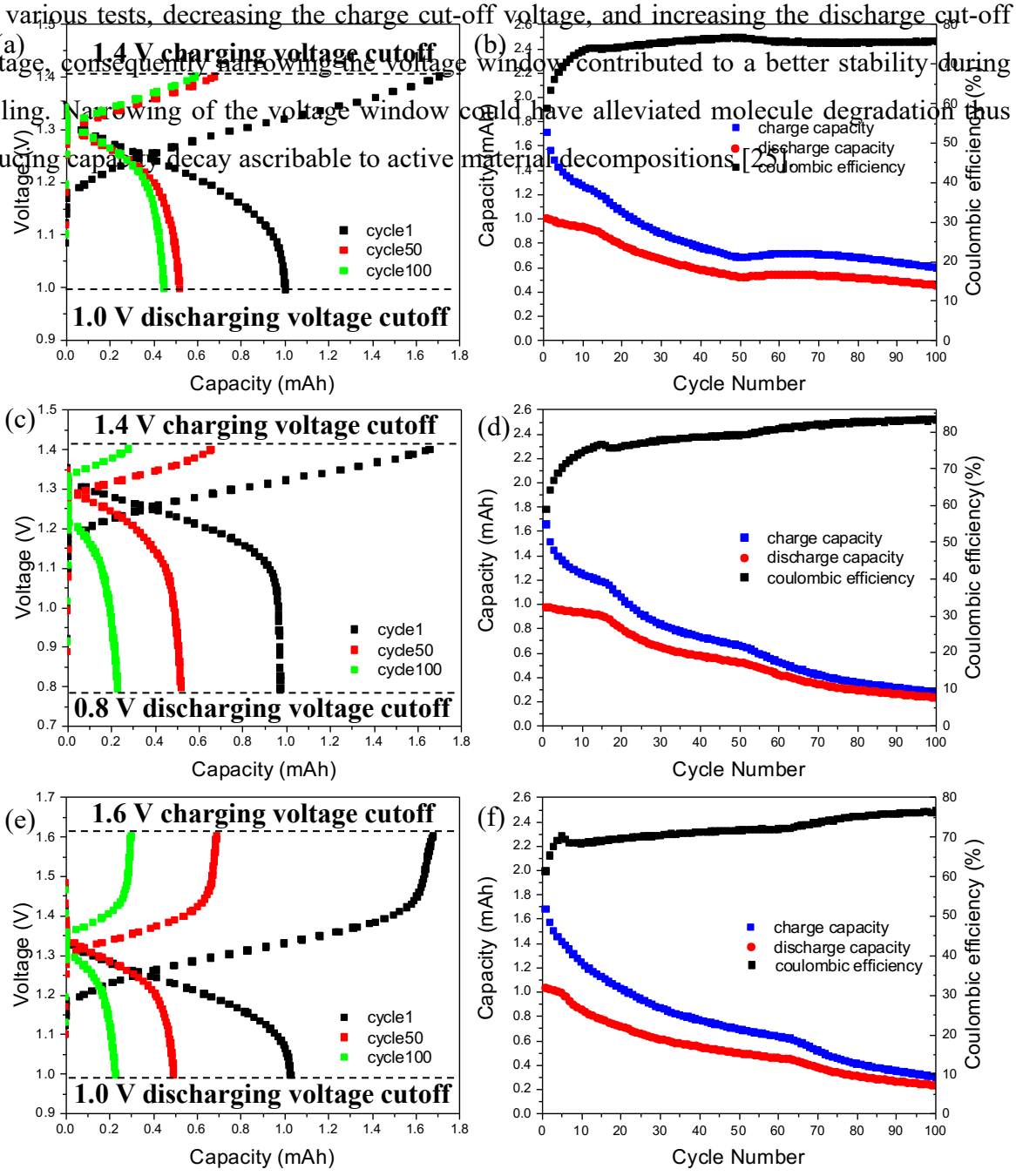

Fig. 4. Demonstration of full flow battery performance of 3 mM combined RIBOTEMPO molecule at current density of 2.5 mA cm^{-2}, exhibiting galvanostatic charge-discharge profiles during the 1^{st}, 50^{th}, and 100^{th} cycles as well as cycling performances and coulombic efficiencies. Condition: (a), (b) at cut-off voltage of 1.0 V - 1.4 V, (c), (d) at cut-off voltage of 0.8 V - 1.4 V and (e), (f) cut-off voltage of 1.0 V - 1.6 V.

Interestingly, battery cycling performance of the combined molecule demonstrated a better stability and long cycle life, in comparison to when a solution-mixture of riboflavin and TEMPO molecules was utilized as the electrolyte. This may be due to the steric effect as a result of combining the two molecules, hindering nucleophilic attacks thus reducing the decomposition rate [33]. Figure S9 displays the battery performance when the mixed solution was employed as both negolyte and posolyte. Figure S9a shows representative voltage vs time curves for the 5^{th} - 10^{th} cycles whereas Figure S9b displays the voltage-capacity profile exhibiting an initial charge capacity of 887.8 mAh. It demonstrated around 30 charge/discharge cycles with a coulombic efficiency of 85% and a very low capacity retention rate of 5% after the 30 cycles (Figure S9c). Moreover, Figure S9d delineates a declining trend in energy and voltage efficiency during battery cycling. The voltage efficiency initially at 93% decreased to 46% after 30 cycles. Similarly, energy efficiency reduced to 42% after 30 cycles from the initial 72%. This could have been as result of faster decomposition of the redox active materials during cycling which led to increased internal resistance in the cell stack [44].

Further battery test runs of the combined molecule at a higher concentration (0.02 M) and higher current density of 25 mA cm^{-2} exhibited 1000 consecutive charge/discharge cycles with around 80% coulombic efficiency as shown in Figure S10. In addition, flow battery testing employing 0.5 M RIBOTEMPO and 1.5 M nicotinamide in 1.5 M NaCl at current density of 40 mA cm^{-2} displayed 120 consecutive charge and discharge cycles, achieving a coulombic efficiency of 90 % as shown in Figure S11. Altogether, this battery chemistry presents various advantages in comparison to the reported symmetric aqueous RFBs based on organic molecules (Table S1). It offers a higher voltage, higher current density as well as comparable cycling performance, efficiencies, and energy density. Besides, low-cost and easily available precursors are utilized in synthesis of the electroactive material via a simple one pot/step method. Therefore, this battery displays attractive features and thus represents potential in advancing symmetric aqueous organic RFBs.

3.3.Stability of the combined molecule

In all battery cycling tests, the charge and discharge plateaus shifted from around 1.23 V in the first cycles to higher values during cycling as shown in Fig. 3a, Fig. 4a, 4c and Fig. 4e, indicating decomposition/modification of the redox active species [45]. Capacity fade in organic redox flow batteries is mostly associated with decomposition of the organic redox active molecule [46]. In our case, the capacity decay is probably caused by decomposition of the RIBOTEMPO redox active molecule or side reactions during battery cycling process. Generally, stability issues as a consequence of the redox active molecule degradation, is the utmost challenge hindering further developments of organic redox flow batteries. Therefore, to address this issue, there is need to understand the decomposition mechanism of these organic molecules so as to foster further development and advancement of these promising technologies [46,47,48,49]. Hence, to evaluate the decomposition of the RIBOTEMPO molecule during battery cycling various tests were carried out. Thenceforth, the decomposition mechanisms were proposed.

(a) Posolyte-TEMPO acidification:

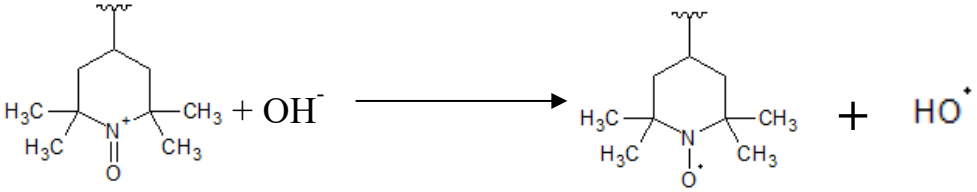

(b) TEMPO: disproportionation reaction in acid

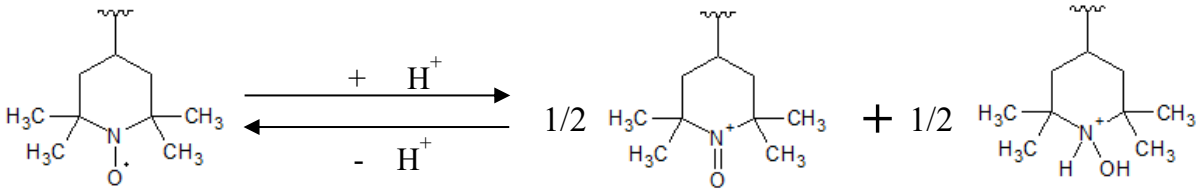

(c) TEMPO+: chemical reduction with OH^-

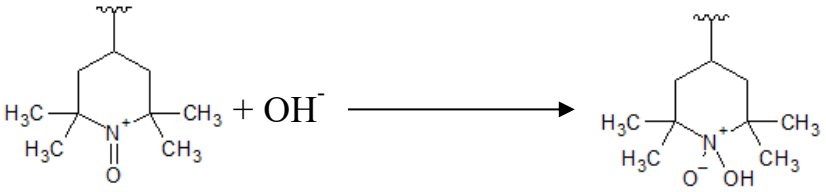

(d) Alloxazine hydrolysis

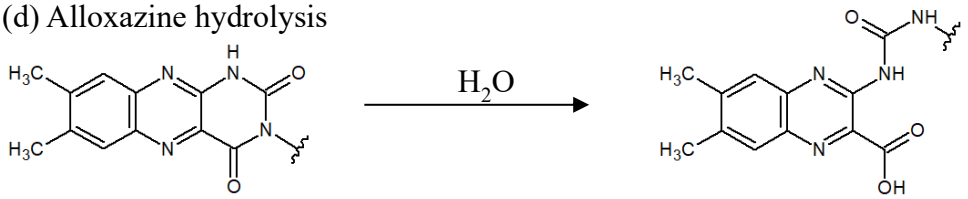

Fig. 5. Illustration of the proposed decomposition mechanisms for RIBOTEMPO molecule.

To get a clear understanding of the decomposition products of the electrolytes, the negolyte and posolyte were collected after 100 charge/discharge cycles. Subsequently, several studies of the spent electrolyte, i.e., electrolyte after cycling were conducted. Figure S12a shows the CV of the spent posolyte in comparison to that of fresh one. It displays decrease in the current peaks of the high potential zone redox couple. Besides this, the pH of the posolyte decreased from neutral pH (6.55) as shown in Figure S12d (fresh electrolyte) to a low pH (pH=1.44) as shown in Figure S12c. The decrease in pH led to formation of an acidic solution, which resulted in positive shifts in potential peaks associated with lower potential zone redox couple. The low potential zone redox couple undergoes a proton dependent redox reaction thus change in pH leads to shifts in the thermodynamic potential (Figure S12b). During cycling, the resulting decrease in pH is attributed to the oxoammonium cation (TEMPO+) consuming OH^- ions to form TEMPO and an hydroxide radical as shown in Fig. 5a. This phenomenon leads to two conditions. Firstly, the produced hydroxyl radical can react with TEMPO causing further decomposition. Secondly, disproportionation reaction in which TEMPO reacts with H^+ will be favoured following the decrease in pH, resulting to formation of two TEMPO derivatives as shown in Fig.5b. The second product shown in Fig. 5b is chemically irreversible, thus effectuating the decrease in the amount of redox active material. In basic conditions, TEMPO+ chemically reacts with OH^- ions (available in high concentrations) to form TEMPO as shown in Fig. 5c. This reduction reaction is chemically irreversible in basic condition, explaining the absence of the reduction peak of the higher potential zone redox couple as shown Figure S7b. The above circumstances led to decrease in concentration of redox active material in the posolyte, eventually, catalysing capacity decay in the RIBOTEMPO symmetric battery. This decomposition of posolyte (TEMPO part) of the combined molecule is in agreement with previous studies done on stability of TEMPO molecule in aqueous solution as reported in other literatures [32,50,51].

On the other hand, an increase in pH bringing about formation of an alkaline solution (pH=11.60) was observed during post cycling analysis of the spent negolyte as shown in Figure S12e. The change in pH led to small negligible shifts in the potential peak associated with the low potential redox couple. Also, the redox peaks associated with TEMPO part of the molecule

became chemically irreversible. The decomposition of riboflavin part was also observed as shown in Fig. 5d, which is in consensus with the previous literatures [52,53,54]. The alkaline condition (pH 11.60) of the negolyte during cycling is believed to have favoured hydrolysis of the riboflavin part [55]. Riboflavin is believed to undergo a ring opening nucleophilic attack initiated by water to form a redox-inactive molecule as shown in MALDI-TOF mass spectra in Figure S13 leading to loss of electroactive material [52]. Also, the mass spectra in Figure S14 confirm molecule decomposition as shown by presence of fragment ions of lumichrome and lumiflavin associated with riboflavin degradation [56]. The analysis of the spent electrolytes revealed modification/decomposition of the molecule during battery cycling as indicated by NMR and UV-Vis spectra shown in Figure S15. The UV-Vis spectra display change/shift in posolyte absorption peaks at lower wavelength suggesting posolyte degradation. Also, the negolyte spectrum exhibits minor changes in absorption peak's height suggesting reduced concentration as a result of molecule degradation. The NMR spectra also indicates possible decomposition. Various changes can be seen, majorly, there is appearance of singlet peaks associated with OH protons at $\delta = 2.6$ and 1.8 ppm for negolyte and posolyte respectively as shown in Figure S15b [57]. Relatedly, RIBOTEMPO molecule (mass spectra shown in Figure S16) undergoes decomposition reactions allied to that of its precursors (mass spectra in Figure S17) [50, 52]. This finding conforms with earlier results, whereby, modification/decomposition of the redox active molecules was revealed by shift in charge/discharge plateaus during cycling. To further identify the origins of the capacity decay, the electrolytes were refreshed after 100 cycles of battery cycling. Whereas refreshing the negolyte didn't show any significant capacity recovery, refreshing the posolyte after 100 cycles led to about 90% recovery of its original capacity as shown in Fig. 6. This gave a clear indication that posolyte decomposition is the main cause of capacity fade during cycling.

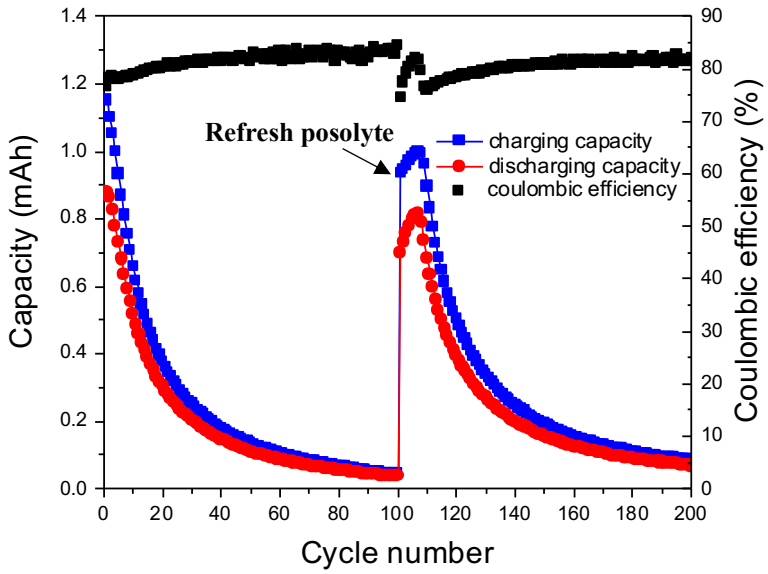

Fig. 6. The cycling performance and coulombic efficiency of combined molecule, when the posolyte was refreshed at 100th cycle.

Based on the above observation, we can conclude that RIBOTEMPO decomposition is the main cause of capacity loss during cycling in this battery chemistry. Evidently, capacity loss is majorly associated with the decomposition of posolyte/TEMPO part of the combined molecule. Whereas, decomposition of the negolyte (riboflavin part of the molecule) was also observed, it's considered not a major cause of the capacity fade observed. Attempt to improve the stability of the molecule using a phosphate buffer solution, so as to maintain a neutral pH electrolyte did not yield significant improvement in capacity retention as shown in Figure S18. Schubert et al. made a comparable observation on their study of bipolar VIOTEMP molecule in aqueous flow battery [21]. Necessarily, molecular modification and replacing TEMPO with other stable amine based molecule such as dopamine to aid solve this stability issue is in consideration.

4. Conclusion

In summary, the RIBOTEMPO combined molecule was successfully synthesized and demonstrated as bifunctional redox active material for symmetric aqueous redox flow battery. The molecule was prepared using low cost commercially available precursors via a simple one pot synthesis method. The molecule is soluble in water and enjoys the merits of aqueous redox flow batteries. This battery chemistry also enjoys low cost and environmental-safe benefits owing to its utilisation of pH-neutral supporting electrolyte as well as an inexpensive anion exchange membrane. Both flow battery testing and CV results confirmed that the RIBOTEMPO flow battery system had a higher cell voltage than previous studies on symmetric aqueous organic systems. The RIBOTEMPO system demonstrated a cell voltage of around 1.23 V and over 100 stable charge/discharge cycles with a coulombic efficiency of nearly 80%. Examination of the spent electrolytes revealed decomposition of the RIBOTEMPO molecule which was the cause of capacity loss in battery performance. This work provides a pathway to explore and design many bipolar molecules to facilitate development of a high-performance symmetric aqueous flow battery.

Acknowledgement

The work described in this paper was fully supported by a grant from the Research Grants Council of the Hong Kong Special Administrative Region, China (Project No. T23-601/17-R). We also thank Biosciences Central Research Facility of HKUST for assistance in the mass

spectrometry experiments. Research at the Argonne National Laboratory was funded by the U.S. Department of Energy (DOE), Vehicle Technologies Office under Contract No. DE-AC02-06CH11357. Support from Tien Duong of the U.S. DOE's Office of Vehicle Technologies Program is gratefully acknowledged.

References

[1] Key World Energy Statistics 2020, OECD Publishing, Paris, 2020.

[2] K. Solaun, E. Cerdá, Climate change impacts on renewable energy generation. A review of quantitative projections, Renew. Sustain. Energy. Rev. 116 (2019), 109415.

[3] R. Chen, S. Kim, Z. Chang, Redox flow batteries: fundamentals and applications, Redox: Principles and Advance Applications. (2017), 103-118.

[4] F. Díaz-González, A. Sumper, O. Gomis-Bellmunt, R. Villafáfila-Robles, A review of energy storage technologies for wind power applications, Renew. Sustain. Energy. Rev. 16 (2012), 2154-2171.

[5] G.L. Soloveichik, Battery technologies for large-scale stationary energy storage, , Annu. Rev. Chem. Biomol. Eng. 2 (2011), 503-527.

[6] M.L. Perry, A.Z. Weber, Advanced redox-flow batteries: a perspective, J. Electrochem. Soc. 163 (2015), A5064.

[7] W. Wang, Q. Luo, B. Li, X. Wei, L. Li, Z. Yang, Recent progress in redox flow battery research and development, Adv. Funct. Mater. 23 (2013), 970-986.

[8] W. Wang, V. Sprenkle, Redox flow batteries go organic, Nat. Chem. 8 (2016), 204-206.

[9] P. Leung, X. Li, C.P. De León, L. Berlouis, C.J. Low, F.C. Walsh, Progress in redox flow batteries, remaining challenges and their applications in energy storage, RSC Adv. 2 (2012), 10125-10156.

[10] E. Sánchez-Díez, E. Ventosa, M. Guarnieri, A. Trovò, C. Flox, R. Marcilla, F. Soavi, P. Mazur, E. Aranzabe, R. Ferret, Redox flow batteries: Status and perspective towards sustainable stationary energy storage, J. Power Sources. 481 (2021), 228804.

[11] J. Luo, B. Hu, M. Hu, Y. Zhao, T.L. Liu, Status and prospects of organic redox flow batteries toward sustainable energy storage, ACS Energy Lett. 4 (2019), 2220-2240.

[12] Q. Chen, L. Eisenach, M.J. Aziz, Cycling analysis of a quinone-bromide redox flow battery, J. Electrochem. Soc. 163 (2015), A5057.

[13] M. Guarnieri, P. Mattavelli, G. Petrone, G. Spagnuolo, Vanadium redox flow batteries: Potentials and challenges of an emerging storage technology, IEEE Ind. Electron. Mag. 10 (2016), 20-31.

[14] P. Geysens, Y. Li, I. Vankelecom, J. Fransaer, K. Binnemans, Highly soluble 1, 4-diaminoanthraquinone derivative for nonaqueous symmetric redox flow batteries, ACS Sustain. Chem. Eng. 8 (2020), 3832-3843.

[15] R.A. Potash, J.R. McKone, S. Conte, H.D. Abruña, On the benefits of a symmetric redox flow battery, J. Electrochem. Soc. 163 (2015), A338.

[16] T. Hagemann, J. Winsberg, B. Häupler, T. Janoschka, J.J. Gruber, A. Wild, U.S. Schubert, A bipolar nitronyl nitroxide small molecule for an all-organic symmetric redox-flow battery, NPG Asia Mater. 9 (2017), e340.

[17] T. Ma, Z. Pan, L. Miao, C. Chen, M. Han, Z. Shang, J. Chen, Porphyrin-Based Symmetric Redox-Flow Batteries towards Cold-Climate Energy Storage, Angewandte Chemie. 130 (2018), 3212-3216.

[18] G.D. Charlton, S.M. Barbon, J.B. Gilroy, C.A. Dyker, A bipolar verdazyl radical for a symmetric all-organic redox flow-type battery, J. Energy Chem. 34 (2019), 52-56.

[19] K.H. Hendriks, C.S. Sevov, M.E. Cook, M.S. Sanford, Multielectron Cycling of a low-potential anolyte in alkali metal electrolytes for nonaqueous redox flow batteries, ACS Energy Lett. 2 (2017), 2430-2435.

[20] J. Winsberg, C. Stolze, S. Muench, F. Liedl, M.D. Hager, U.S. Schubert, TEMPO/phenazine combi-molecule: a redox-active material for symmetric aqueous redox-flow batteries, ACS Energy Lett. 1 (2016), 976-980.

[21] T. Janoschka, C. Friebe, M.D. Hager, N. Martin, U.S. Schubert, An approach toward replacing vanadium: a single organic molecule for the anode and cathode of an aqueous redox-flow battery, ChemistryOpen. 6 (2017), 216-220.

[22] V. Singh, S. Kim, J. Kang, H.R. Byon, Aqueous organic redox flow batteries, Nano Res. 12 (2019), 1988-2001.

[23] R.P. Fornari, M. Mesta, J. Hjelm, T. Vegge, P. de Silva, Molecular engineering strategies for symmetric aqueous organic redox flow batteries, ACS Mater. Lett. 2 (2020), 239-246.

[24] A. Orita, M.G. Verde, M. Sakai, Y.S. Meng, A biomimetic redox flow battery based on flavin mononucleotide, Nat. Commun. 7 (2016), 1-8.

[25] T. Liu, X. Wei, Z. Nie, V. Sprenkle, W. Wang, A total organic aqueous redox flow battery employing a low cost and sustainable methyl viologen anolyte and 4-HO-TEMPO catholyte, Adv. Energy Mat. 6 (2016), 1501449.

[26] B. Liu, X. C.W. Tang, H. Jiang, G. Jia, T. Zhao, Carboxyl-functionalised TEMPO catholyte enabling high-cycling-stability and high-energy-density aqueous organic redox flow batteries, ACS. Sustain. Chem. Eng. 9 (2021), 6258-6265.

[27] Y. Ding, C. Zhang, L. Zhang, Y. Zhou, G. Yu, Molecular engineering of organic electroactive materials for redox flow batteries, Chem. Soc. Rev. 47 (2018), 69-103.

[28] S. Er, C. Suh, M.P. Marshak, A. Aspuru-Guzik, Computational design of molecules for an all-quinone redox flow battery, Chem. Sci. 6 (2015), 885-893.

[29] L. Xie, J. Cheng, Z. Luo, G. Lu, Mannich reaction of indole with cyclic imines in water, Tetrahedron Lett. 59 (2018), pp. 457-461.

[30] A.V. Bogdanov, L.I. Musin, A.V. Il'in, V.F. Mironov, Novel 1-Aminomethylisatins: Peculiarities of the Synthesis and the Reaction with Tris (diethylamino) phosphine, J. Heterocycl. Chem. 51 (2014), 1027-1030.

[31] N. Azizi, L. Torkiyan, M.R. Saidi, Highly efficient one-pot three-component Mannich reaction in water catalyzed by heteropoly acids, Org. Lett. 8 (2006), 2079-2082.

[32] J.B. Gerken, Y.Q. Pang, M.B. Lauber, S.S. Stahl, Structural Effects on the pH-Dependent Redox Properties of Organic Nitroxyls: Pourbaix Diagrams for TEMPO, ABNO, and Three TEMPO Analogs, J. Org. Chem. 83 (2017), 7323-7330.

[33] K. Lin, R. Gómez-Bombarelli, E.S. Beh, L. Tong, Q. Chen, A. Valle, A. Aspuru-Guzik, M.J. Aziz, R.G. Gordon, A redox-flow battery with an alloxazine-based organic electrolyte, Nat. Energy. 1 (2016), 1-8.

[34] N. Elgrishi, K.J. Rountree, B.D. McCarthy, E.S. Rountree, T.T. Eisenhart, J.L. Dempsey, A practical beginner's guide to cyclic voltammetry, J. Chem. Educ. 95 (2018), 197-206.

[35] A.J. Bard, L.R. Faulkner, Fundamentals and applications, Electrochemical Methods. 2 (2001), 580-632.

[36] T.C. Chan, H.T. Li, K.Y. Li, Effects of shapes of solute molecules on diffusion: A study of dependences on solute size, solvent, and temperature, J. Phys.l Chem. B. 119 (2015), 15718-15728.

[37] A. T. Celebi, S. H. Jamali, A. Bardow, T. J. Vlugt, O. A. Moultos, Finite-size effects of diffusion coefficients computed from molecular dynamics: a review of what we have learned so far. Mol. Simul. (2020), 1-15.

[38] A. Mukhopadhyay, H. Zhao, B. Li, J. Hamel, Y. Yang, D. Cao, A. Natan, H. Zhu, Abundant organic dye as an anolyte for aqueous flow battery with multielectron transfer, ACS Appl. Energy Mater. 2 (2019), 7425-7437.

[39] D. V. Frost, The effect of nicotinamide of the solubility of riboflavin in water. *J. Am. Chem. Soc.* 69 (1947), 1064–1065.

[40] R. E. Coffman, D. O. Kildsig, Effect of nicotinamide and urea on the solubility of riboflavin in various solvents. J. Pharm. Sci. 85 (1996), 951–954.

[41] A. A. Rasool, A. A. Hussain, L. W. Ditter, Solubility enhancement of some water-insoluble drugs in the presence of nicotinamide and related-compounds. J. Pharm. Sci. 80 (1991), 387–393.

[42] M. P. Evstigneev, V. P. Eustigneev, A. A. H. Santiago, D. B. Davies, Effect of a mixture of caffeine and nicotinamide on the solubility of vitamin (B-2) in aqueous solution. Eur. J. Pharm. Sci. 28 (2006), 59–66.

[43] J. Chai, X. Wang, A. Lashgari, C.K. Williams, J. Jiang, A pH-Neutral, Aqueous Redox Flow Battery with a 3600-Cycle Lifetime: Micellization-Enabled High Stability and Crossover Suppression, ChemSusChem. 13 (2020), 4069-4077.

[44] Z. Yang, L. Tong, D.P. Tabor, E.S. Beh, M. Goulet, D. De Porcellinis, A. Aspuru-Guzik, R.G. Gordon, M.J. Aziz, Alkaline benzoquinone aqueous flow battery for large-scale storage of electrical energy, Adv. Energy Mater. 8 (2018), 1702056.

[45] Y.Y. Lai, X. Li, K. Liu, W. Tung, C. Cheng, Y. Zhu, Stable low-cost organic dye anolyte for aqueous organic redox flow battery, ACS Appl. Energy Mat. 3 (2020), 2290-2295.

[46] D.G. Kwabi, Y. Ji, M.J. Aziz, Electrolyte lifetime in aqueous organic redox flow batteries: a critical review, Chem. Rev. 120 (2020), 6467-6489.

[47] X. Wei, W. Pan, W. Duan, A. Hollas, Z. Yang, B. Li, Z. Nie, J. Liu, D. Reed, W. Wang, Materials and systems for organic redox flow batteries: status and challenges, ACS Energy Lett. 2 (2017), 2187-2204.

[48] K. Wedege, E. Dražević, D. Konya, A. Bentien, Organic redox species in aqueous flow batteries: redox potentials, chemical stability and solubility, Sci. Rep. 6 (2016), 1-13.

[49] F.R. Brushett, M.J. Aziz, K.E. Rodby, On lifetime and cost of redox-active organics for aqueous flow batteries, ACS Energy Lett. 5 (2020), 879-884.

[50] A. Orita, M.G. Verde, M. Sakai, Y.S. Meng, The impact of pH on side reactions for aqueous redox flow batteries based on nitroxyl radical compounds, J. Power Sources. 321 (2016), 126-134.

[51] Y. Ma, C. Loyns, P. Price, V. Chechik, Thermal decay of TEMPO in acidic media via an N-oxoammonium salt intermediate, Org. Biomol. Chem. 9 (2011), 5573-5578.

[52] S.B. Smith, T.C. Bruice, Mechanisms of isoalloxazine (flavine) hydrolysis, J. Am. Chem. Soc. 97 (1975), 2875-2881.

[53] A.R. Surrey, F.C. Nachod, Alkaline hydrolysis of riboflavin, J. Am. Chem. Soc. 73 (1951), 2336-2338.

[54] T. Harayama, Y. Tezuka, T. Taga, F. Yoneda, Hydrolysis products of flavins (isoalloxazines), J. Chem. Soc. Perkin Trans. 1. (1987), 75-83.

[55] J. Koziol, B. Tyrakowska, F. Müller, The structure of covalent hydrates of alloxazines. A reinvestigation, Helv. Chim. Acta. 64 (1981), 1812-1817.

[56] J.S. Stanojević, J.B. Zvezdanović, D.Z. Marković, Riboflavin degradation in the presence of quercetin in methanol under continuous UV-B irradiation: the ESI–MS–UHPLC analysis, Monatshefte für Chemie-Chemical Monthly. 146 (2015), 1787-1794.

[57] E. Pretsch, P. Bühlmann, M. Badertscher, ^{1}H NMR Spectroscopy. Structure Determination of Organic Compounds, Springer, (2020), 167-254.

Biography

Gabriel Sikukuu Nambafu received his Bachelor's degree in Industrial Chemistry with Management from Kenyatta University, Kenya (2013), and M.S. degree in Materials Science and Engineering from Kangwon National University, South Korea in 2017. He is now a Ph.D. candidate in Chemical and Biomolecular Engineering at the Hong Kong University of Science and Technology under the supervision of Prof. Minhua Shao. His main research interests is on advanced materials for organic redox flow batteries.

Kumar Siddharth received his Bachelor's degree in the Chemical Engineering from National Institute of Technology Durgapur, India (2016), and Ph.D. in Chemical and Biomolecular Engineering from the Hong Kong University of Science and Technology in 2020. He is now a postdoctoral fellow in the Hong Kong University of Science and Technology under the supervision of Prof. Minhua Shao. His research is focused on catalyst development and mechanistic study of ammonia oxidation reaction.

Cheng ZHANG received her Bachelor's degree from Northwestern Polytechnical University, China, and she completed her Master and PhD study from the Hong Kong University of Science and Technology. She is now a Postdoctoral fellow in the Hong Kong University of Science and Technology under the supervision of Prof. Tianshou Zhao. Her research area includes the systematic design and optimization of organic and inorganic redox flow batteries.

Tianshou Zhao received his Bachelor's and Master's degrees from Tianjin University, China, and completed his Ph.D. study in the University of Hawaii at Manoa, USA. He is now Cheong Ying Chan Professor of Engineering and Environment , Chair Professor in the Department of Mechanical Engineering and Aerospace Engineering, Director of Energy Institute at the Hong Kong University of Science and Technology (HKUST) and a member of the Chinese Academy of Sciences (CAS). Prof. Zhao combines his expertise in research and technological innovation with a commitment to creating clean energy production and storage devices for a sustainable future. He has made seminal contributions in the areas of fuel cells, advanced batteries, multi-scale multiphase heat and mass transport with electrochemical reactions, and computational modelling.

Qing Chen received his Bachelor's degree from Zhejiang University, and his Ph.D. in Materials Science from Arizona State University. He was a postdoctoral researcher at Harvard University before joining the Hong Kong University of Science and Technology. He is now a Professor in the Department of Mechanical and Aerospace Engineering and a board member of Energy Institute of the Hong Kong University of Science and Technology. He also holds a joint appointment at the Department of Chemistry. Prof. Chen's research applies materials science and electrochemistry to understand and control self-organization at nanoscales. The same knowledge set guides the design of electrochemical devices such as redox flow batteries for grid-scale electricity storage.

Khalil Amine is an Argonne Distinguished Fellow and Manager of the Advanced Battery Technology programs at Argonne National Laboratory, where he is responsible for directing the research and development of advanced materials and battery systems for HEV, PHEV, EV, satellite, military, and medical applications. Dr. Amine currently serves as a committee member of the U.S. National Research Consul, U.S. Academy of Sciences, on battery-related technologies. He is also the president of IMLB LLC, an international automotive battery conference.

Minhua Shao earned his B.S. (1999) and M.S. (2002) degrees in Chemistry from Xiamen University, and a Ph.D. degree in Materials Science and Engineering from the State University of New York at Stony Brook (2006). He received the Supramaniam Srinivasan Young Investigator Award from the ECS Energy Technology Division (2014). He is now a Professor in the Department of Chemical and Biological Engineering and Associate Director of Energy Institute of the Hong Kong University of Science and Technology. His research is mainly focused on electrocatalysis, fuel cells, and advanced batteries.